Anal. Bioanal. Electrochem., Vol. 8, No. 2, 2016, 169-183

Analytical & Bioanalytical Electrochemistry

2016 by CEE
www.abechem.com

Full Paper

Electrocatalytic Oxidation of Cisapride at Carbon Paste Electrode Modified with Copper Sulfide Nanostructures

Ghasem Karim-Nezhad*and Sara Pashazadeh

Department of Chemistry, Payame Noor University, PO BOX 19395-3697 Tehran, Iran

*Corresponding Author, Tel.: +98 44 36349868; Fax: +98 44 36332556

E-Mail: g.knezhad@gmail.com

Received: 11 November 2015 / Accepted: 15 March 2016 / Published online: 31 March 2016

Abstract- In the present study, a new carbon paste electrode chemically modified with copper sulfide nanostructures is constructed and used for the catalytic oxidation of cisapride. The voltammetric behavior and electrochemical reaction mechanism of cisapride have been investigated at modified electrode using cyclic voltammetry (CV), steady state polarization and differential pulse voltammetry. In CV studies, no oxidation response of cisapride can be seen at the unmodified electrode, but at the copper sulfide nanostructures modified carbon paste electrode (CSN-MCPE), a large anodic peak appears, indicating that the anodic oxidation of cisapride could be catalyzed at CSN-MCPE. This proves that the copper sulfide nanostructures bear the main role in electrocatalytic oxidation of cisapride. The kinetic parameter such as the electron transfer coefficient (α) and exchange current density (j_0) for the modified electrode were calculated. The differential pulse peak current varied linearly with the concentration of cisapride in range of 9×10^{-8} to 15×10^{-6} mol L^{-1}. The modified electrode can be prepared very easy and renewed in its surface by simple polishing. The reproducibility of the electrode response, based on six measurements during two month, was 3.23% for the slope of the calibration curve.

Keywords- Cisapride, Modified carbon paste electrode, Copper sulfide nanostructures, Electrocatalytic oxidation, Kinetic study

1. INTRODUCTION

Cisapride, 4-amino-5-chloro-N-{1-[3-(4-fluorophenoxy)-propyl]-3-methoxy-piperidin-4-yl}-2-methoxy-benzamide is widely used for the treatment of some gastro-oesophageal diseases such as oesophageal reflux, non-ulcer dyspepsia [1]; caused by disordered motility

[2-6]. Several methods have been developed for the study of the drug including high-performance liquid chromatography [7,8], ultraviolet spectrophotometry [9], spectrofluorimetry [10], potentiometric titration [11], voltammetry [12] and polarography [13].

Electrochemical techniques have been proven to be very sensitive to the study of drugs and related molecules. Moreover, the use of chemically modified electrodes in electrochemical methods is widely reported for study of various pharmaceuticals [14,15]. Carbon electrodes may be classified in two sections as homogeneous (glassy carbon, graphite, vitreous carbon, screen printed, fullerens, carbon nanotubes and diamond) and heterogeneous (carbon paste, modified carbon paste) [16]. The ease and speed of preparation and of obtaining a new reproducible surface, low residual current, porous surface, and low cost of carbon paste are some advantages of carbon paste electrode(CPE) over all other carbon electrodes. Therefore, CPE can provide a suitable electrode substrate for preparation of modified electrodes [17]. Modification of the paste matrix with various transition metal complexes [18–20] were reported in recent years. These electrodes have been widely used in electrochemistry due to their ability to catalyze the redox processes of some molecules of interest, since they facilitate the electron transfer [21].

In the study described here, kinetic study of the electrocatalytic oxidation of cisapride at a copper sulfide nanostructures modified carbon paste electrode (CSN-MCPE) was investigated.

2. EXPERIMENTAL

2.1. Reagent and apparatus

All chemicals used, were from Merck (Darmstadt, Germany) and Sigma Aldrich. Cisapride was received from the Center of Quality Control of Drug, Tehran, Iran. Stock solution of cisapride was prepared to be methanol/water (10:90 V/V) solution and stored at 0–4 ℃. Cisapride working solutions under voltammetric investigations were prepared by dilution of the stock solution.

Electrochemical measurements were carried out in a three-electrode cell using an Autolab electrochemical system (Eco Chemie, Utrecht, the Netherlands) equipped with PGSTAT-12 and GPES software. The three electrode system was used in the measurements, with a bare or chemically modified carbon paste electrode as the working electrode, Ag/AgCl/ saturated KCl as the reference electrode and a platinum wire as the auxiliary electrode. All experiments were carried out at room temperature.

A LEO1430 vp (Carl Zeiss, Germany) scanning electron microscope (SEM) equipped with energy dispersive X-ray spectroscopy (EDXS) was used to surfaces and morphology,

nanostructure properties and chemical composition characterization of the copper sulfide nanostructures.

2.3. Preparation of copper sulfide nanostructures

The procedure for preparation of Cu_2S nanostructures was adapted from Ref. [22]. Self-mosaic flower-like Cu_2S nanostructure was prepared by a two-step hydrothermal process. The original self-assembled Cu_2S nanoflowers were obtained by the following first step. 1g of $CuCl_2.2H_2O$ and 0.8 g of thiourea powders were added into 80 mL ethanol to form yellow–green slurry. The slurry was stirred for 30 min and then transferred into a 100 mL Teflon autoclave. The autoclave was maintained at 160 °C for 6 h and then air-cooled to room temperature. The resulting dark precipitates were washed with distilled water and ethanol several times and then dried at 50 °C under vacuum for 10 h. The self-mosaic Cu_2S sample was prepared by the following second step. Half of the obtained original nanoparticles were added into the other yellow–green slurry and the reaction conditions were the same as those described in the first step, only the $CuCl_2.2H_2O$ and thiourea powders were 0.25 g and 0.2 g respectively.

2.4. Preparation of copper sulfide nanostructures modified carbon paste electrode

The CSN-MCPE was prepared by hand mixing 68% graphite powder, 12% copper sulfide nanostructures and 20% paraffin oil in an agate mortar to get homogeneous carbon paste. Then, paste was packed into the end of a polyethylene syringe (2 mm in diameter). A copper wire inserted into the carbon paste provided an electrical contact. Before each measurement, pushing an excess of paste out of the tube and then polishing the freshly exposed paste with weighing paper obtained a new surface. Also, unmodified carbon paste was prepared in the same way but without adding copper sulfide nanostructures to the mixture. Then, the electrode was placed in 0.1 mol L^{-1} NaOH and the electrode potential was cycled between -250 and 1000 mV (*vs.* Ag/AgCl) at a scan rate of 50 mVs^{-1} for 16 cycles in a cyclic voltammetry regime until a stable voltammogram was obtained. The electrode was rinsed with distilled water, and applied for electrochemical studies. The sample solutions were equilibrated with the electrode surface for 60s before each measurement.

3. RESULTS AND DISCUSSION

3.1. Characterization of copper sulfide nanostructures

The crystal morphologies of the resulting products was characterized by scanning electron microscopy (SEM) and surface elemental analysis was studied by energy dispersive X-ray (EDX) technique. Fig. 1A gives the SEM image of the original Cu_2S nanostructures. It

shows that the Cu_2S nanocrystals are made up of monodisperse structures with a flower-like morphology. The diameter of the nanoflowers is about 1 μm. A high magnification SEM image, shown in the inset of Fig. 1A(b), possesses a nanosheets self-assembled pattern.

Fig. 1B illustrates the elemental composition of the electrode surface respectively. The spectrum shows sharp peaks corresponding to Cu and S, and the atomic ratio of Cu to S is found to be~2:1 within the experimental error. The very weak 'O' peak may be originated from the oxidation of the product exposed to the atmosphere since nanocrystalline material exhibits a high surface to- volume ratio. Also, EDX analysis of Cu_2S revealed one sulfide peak at 2.155 keV.

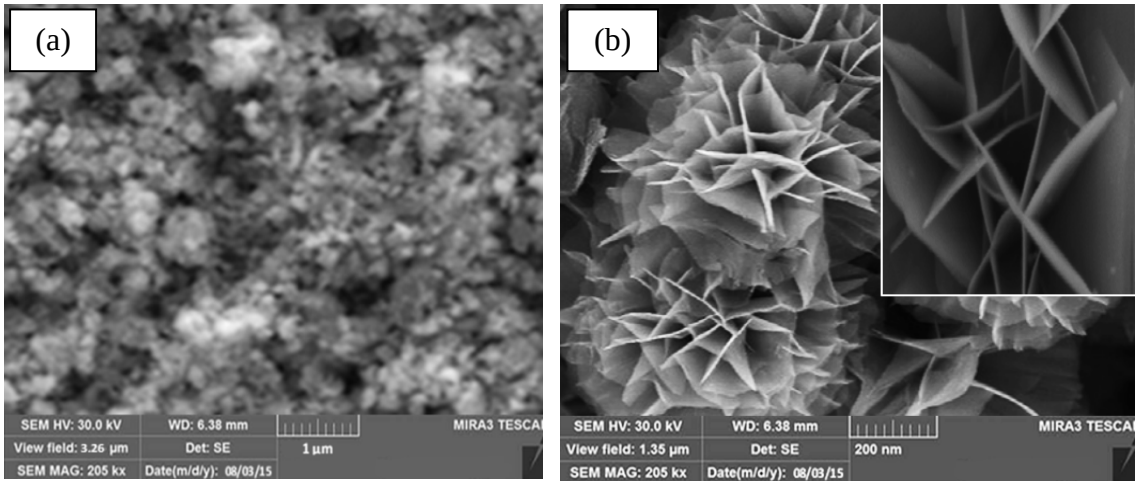

(A)

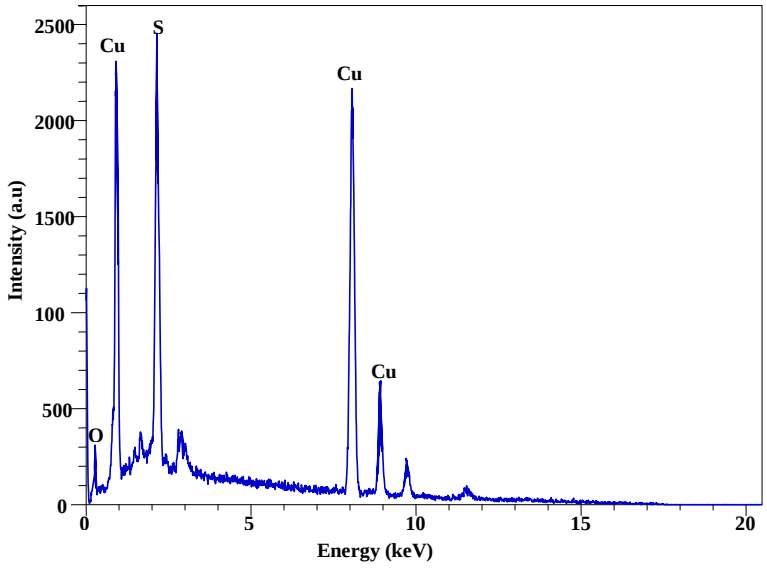

(B)

Fig. 1. (A) SEM images of Cu_2S nanostructures in low (a) and high magnification (b). Inset: the SEM image with higher magnification for the sample, scale bar is 50 nm; **(B)** EDX spectrum of Cu_2S nanostructures sample

3.2. Improvement of the electrode quality of CPE with the modification of copper sulfide nanostructures

The voltammograms of cisapride at unmodified carbon paste and CSN-MCPE in 0.1 mol L^{-1} NaOH solution are shown in Fig. 2. As seen in Fig. 2A any oxidation signal was not exhibited on the CPE. This indicated the electroinactivity of cisapride on the CPE surface. Typical cyclic voltammograms of CSN-MCPE in 0.1 mol L^{-1} NaOH are shown as Fig. 2B where potential sweep rate of 50 mVs^{-1} has been employed. In the absence of cisapride, no peak appears at the CSN-MCPE. While cisapride exhibits high oxidation peak, located at 0.766 V.

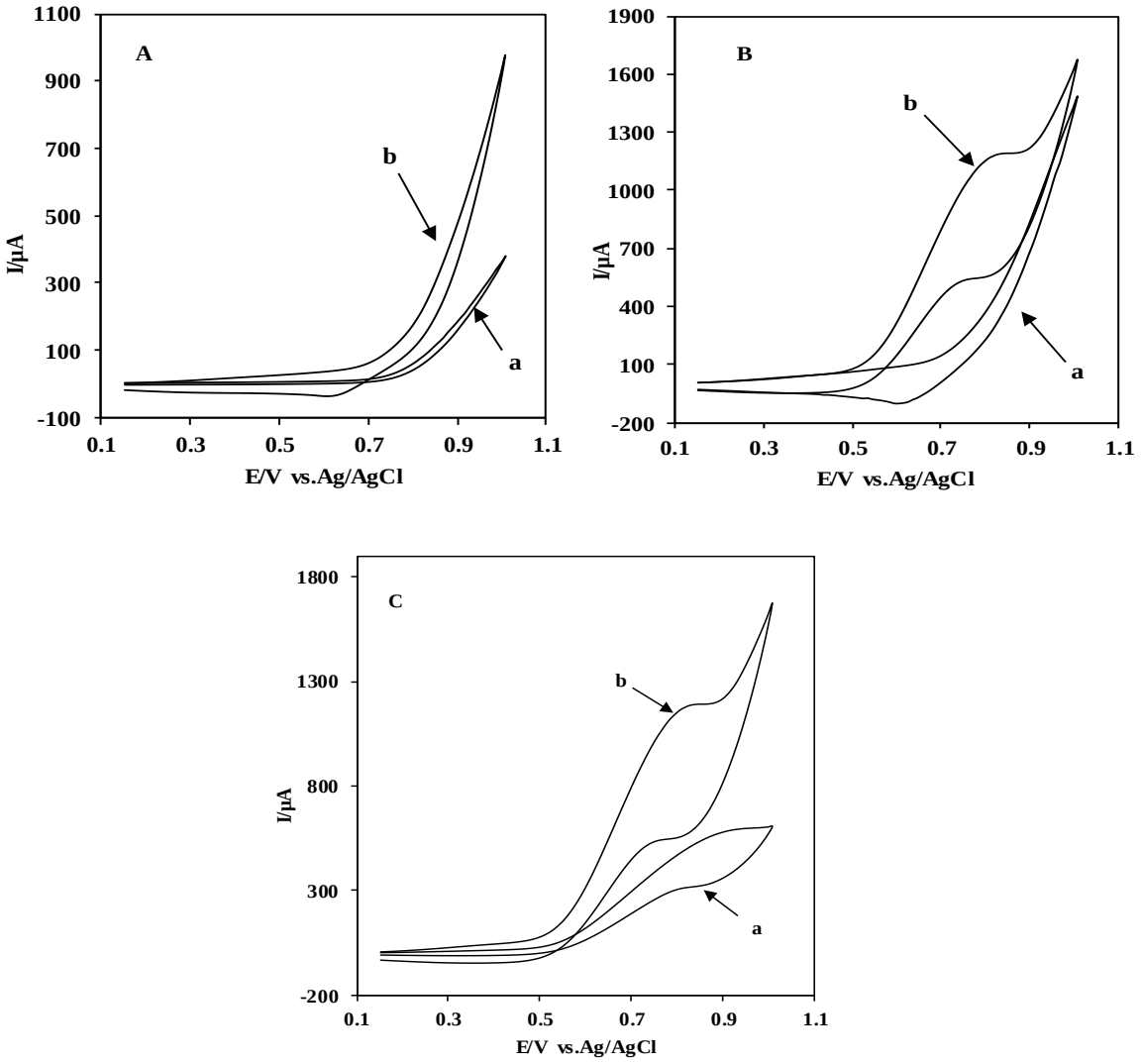

Fig. 2. Cyclic voltammograms of bare CPE (A) and CSN-MCPE; (B) in the absence (curve a) and in the presence (curve b) of 15×10^{-6} mol L^{-1} cisapride; (C) CVs of original Cu_2S MCP and Cu_2S nanostructure MCP electrodes in 0.1 mol L^{-1} NaOH solution in the presence of 15×10^{-6} mol L^{-1} cisapride. Conditions: Supporting electrolyte: 0.1 mol L^{-1} NaOH; scan rate: 50 mV s^{-1}; potential range 150 to 1000 mV *vs*. Ag/AgCl

It showed that no reduction peak was observed in the reverse scan, suggesting that the electrochemical reaction was a totally irreversible process.

The influence of scan rate was investigated in the range of 5-100 mVs^{-1} on the electrochemical behaviour of CSN-MCPE in the presence of cisapride (Fig. 3). A linear relationship was observed between anodic peak current with scan rate (Fig. 4A) indicates an adsorptive redox process, which may be due to the tendency of cisapride to interact with copper ions at the electrode surface [23]. A linear relationship was also observed between log I_p and log ν with a slope of 0.5041(Fig. 4B) which shows the large contribution of adsorption of cisapride to the current flow; in the case of diffusion currents, the slope approaches 0.5[24].

As for a totally irreversible electrode process with adsorption character, the relationship between the peak potential E_p and the scan rate v was followed by the Laviron equation [25].

$$E_p = E^{\circ'} + \left(\frac{2.303RT}{\alpha nF}\right)\log\left(\frac{RTk^{\circ}}{\alpha nF}\right) + \left(\frac{2.303RT}{\alpha nF}\right)\log v \qquad (1)$$

The oxidation peak potential E_p of cisapride shifted linearly with log v in the range of 5–100 mV s^{-1} with the linear regression equation of E_p/V=0.4794+0.0902 log v (mV s^{-1}) (R=0.9971, n=13) (Fig. 4C). Generally, the electron transfer coefficient α was about 0.5 in the totally irreversible electrode process. Therefore, the number of electrons (n) transferred in the oxidation of cisapride was 2. The intercept of E_p *vs.* log I plot was used for calculated of exchange current density. The exchange current density (j_0) evaluated from Tafel plots is 6.21×10^{-7} Acm^{-2}.

The value of k° can be determined from the intercept of the above plot if the value of $E^{\circ'}$ is known. The value of $E^{\circ'}$ in Eq. (1) can be obtained from the intercept of E_p *vs.* ν curve by extrapolating to the vertical axis at ν=0. In our system the intercept for E_p *vs.* log ν plot was 0.4794 and $E^{\circ'}$ was obtained to be 0.5625 V, the k° was calculated to be 1.4963 s^{-1}.

In the cisapride molecule, the possible electrooxidation group was the primary amino group that connected with the phenyl ring. Therefore, its electrochemical reaction was suggested as follows:

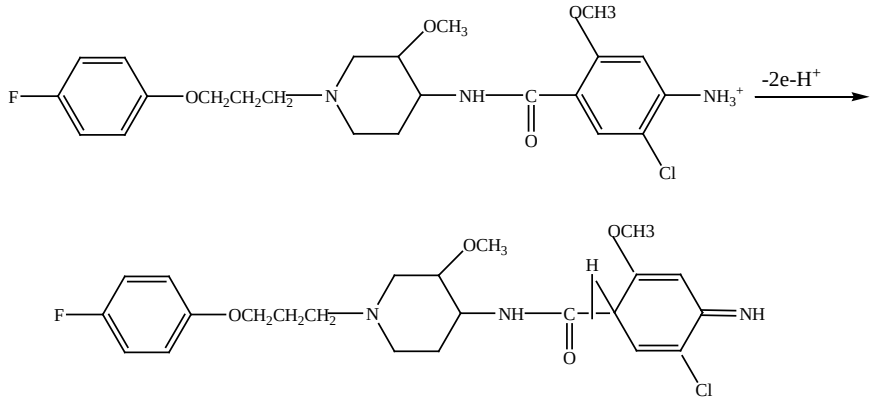

(1)

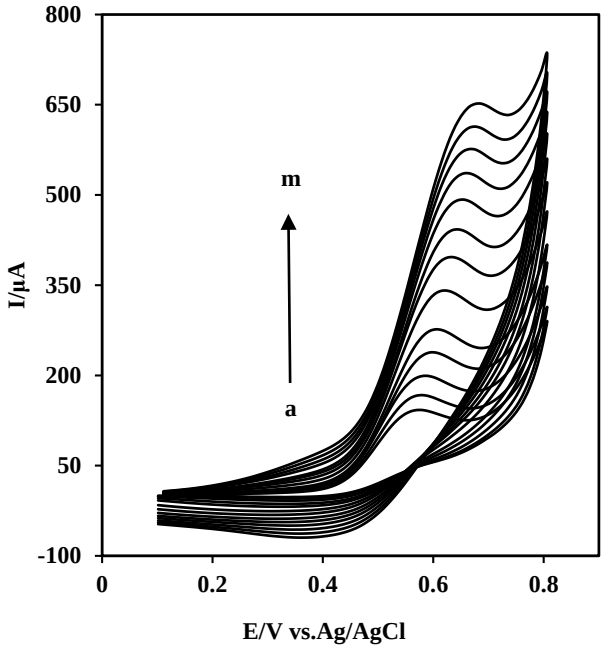

Fig. 3. CVs of CSN-MCPE in 0.1 mol L^{-1} NaOH solution containing 7×10^{-6} mol L^{-1} cisapride at various scan rates; from inner to outer scan rates of 5,7, 10, 15, 20, 25, 30, 40,50, 60, 70, 80, 90, and 100 mV s^{-1}, respectively.

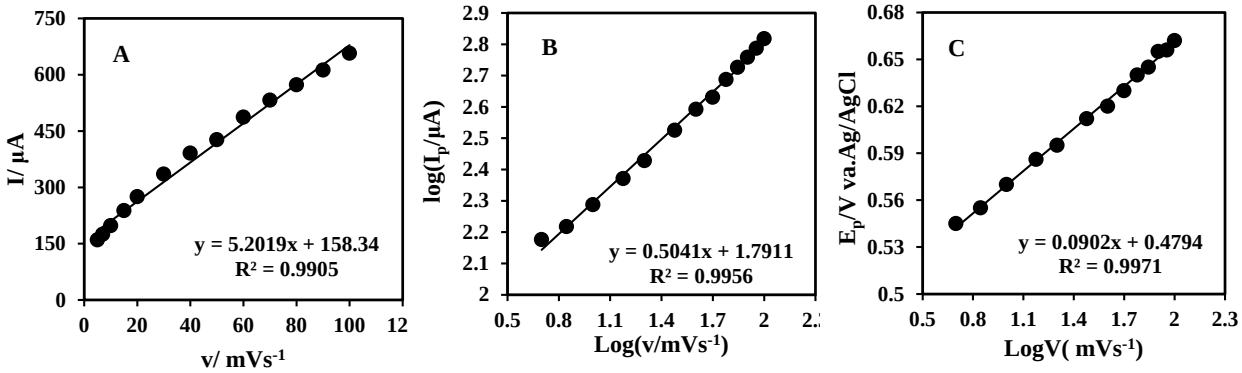

Fig. 4. (A) Dependency of anodic peak current *vs*. scan rate; (B) Plot of logarithm of peak current *vs*. logarithm of scan rate; (C) Plot of variation of peak potential with logarithm of scan rate

3.3. Effect of accumulation time

Fig. 5 shows the plot of anodic peak current *vs*. the accumulation time for 7×10^{-6} mol L^{-1} cisapride solution. The peak current increased with accumulation time up to 60 s, beyond which it leveled off due to the saturation of the active surface of the electrode. Therefore, the

sample solutions were equilibrated with the electrode surface for 60 s before each measurement.

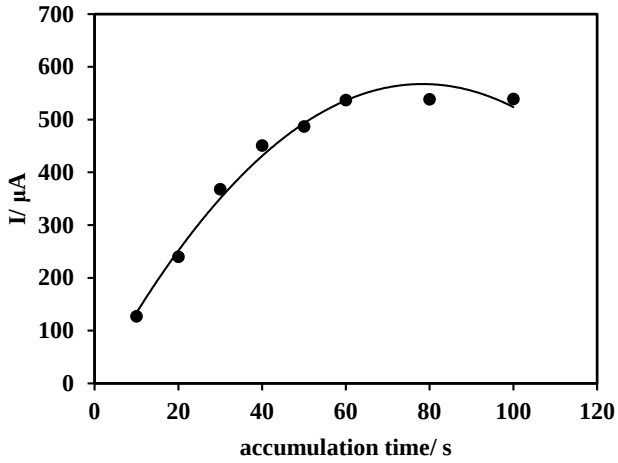

Fig. 5. Influence of the accumulation time on the modified electrodes response using cyclic voltammograms anodic peak currents of 7×10^{-6} mol L^{-1} cisapride in 0.1 mol L^{-1} NaOH solution at scan rate of 50 mV s^{-1}

3.4. Effect of supporting electrolyte

The electrochemical responses of 7×10^{-6} mol L^{-1} cisapride at the CSN-MCPE in different supporting electrolytes such as sodium hydroxide solutions, Phosphate, ammonia - ammonium chloride and Britton-Robinson buffers were investigated. It was found that the oxidation peak of cisapride was well-defined and more sensitive in the NaOH. The cyclic voltammograms of CSN-MCPE electrode were recorded in different concentrations of NaOH solution containing 7×10^{-6} mol L^{-1} cisapride (not shown). It is shown that, the high catalytic peak current is achieved above a NaOH concentration of 0.1 mol L^{-1}. So, 0.1 mol L^{-1} NaOH was chosen as an optimum supporting electrolyte.

3.5. Linear dynamic range of the method

Differential pulse voltammetry (DPV) was used at a scan rate of 20 mVs^{-1}. The dependence of the oxidation peak current (I_{pa} of cisapride) on its concentration was investigated in NaOH solution by DPV. The obtained DPVs at different concentrations of cisapride are shown in Fig. 6. Under optimum conditions, the variation of DPV peak current with cisapride concentration was linear for concentrations ranging from 9×10^{-8} to 15×10^{-6} mol L^{-1}. A comparison was made between the analytical performances of the proposed method with some recently reported methods for determination of cisapride (Table 1). As

show, the linear range and LOD of the proposed method are significantly comparable with previous reports.

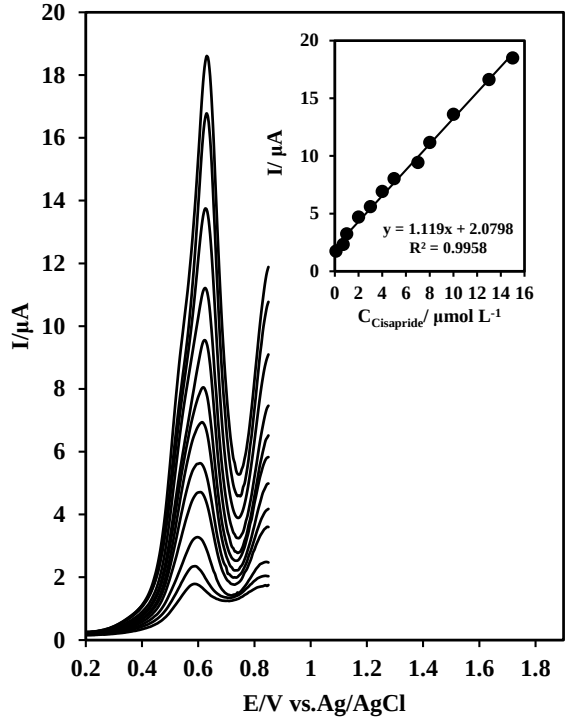

Fig. 6. DPVs of CSN-MCPE for cisapride (9×10^{-8} -15×10^{-6} mol L^{-1}) in NaOH (0.1 mol L^{-1}); scan rate=0.02 V s^{-1}, inset: calibration curve

Table 1 Comparison of major characteristics of different methods for determination of cisapride

Method	Linear range (µM)	LOD (µM)	References
Polarography	1.3×10^{-2} - 8.4×10^{-4}	0.18	[13]
Fluorimetry	8- 160	9.4	[10]
HPLC	0.5- 200	40	[4]
Voltammetry	0.04- 20	0.01	[12]
CSN-MCPE	0.09 - 15	1.01	This work

3.6. Chronoamperometric Study

In order to evaluate the reaction kinetics, the oxidation of cisapride on CSN-MCPE was investigated by chronoamperometry. Fig. 7A shows the recorded chronoamperograms for the modified electrode in the absence and presence of different concentrations of cisapride using

a step potential to 0.58 V. As is obvious, the anodic current increased in the presence of the increasing amounts of the drug. The amount of catalytic current depends on the concentration of cisapride as well as the catalytic rate constant, *K* according to Eq. (2) [26]:

$$I_{cat}/I_d = \lambda^{1/2}\pi^{1/2}(KCt)^{1/2} \quad (2)$$

I_{cat} and I_d are limiting currents in the presence and absence of cisapride, respectively. *C* is the molar concentration of cisapride and t is the elapsed time (s). The value of *K* was calculated for different concentrations of cisapride from the slope of I_{cat}/I_d versus $t^{1/2}$ plot (Fig. 7B). The average value for *K* was found to be 6.04×10^7 cm^3 $mol^{-1}s^{-1}$.

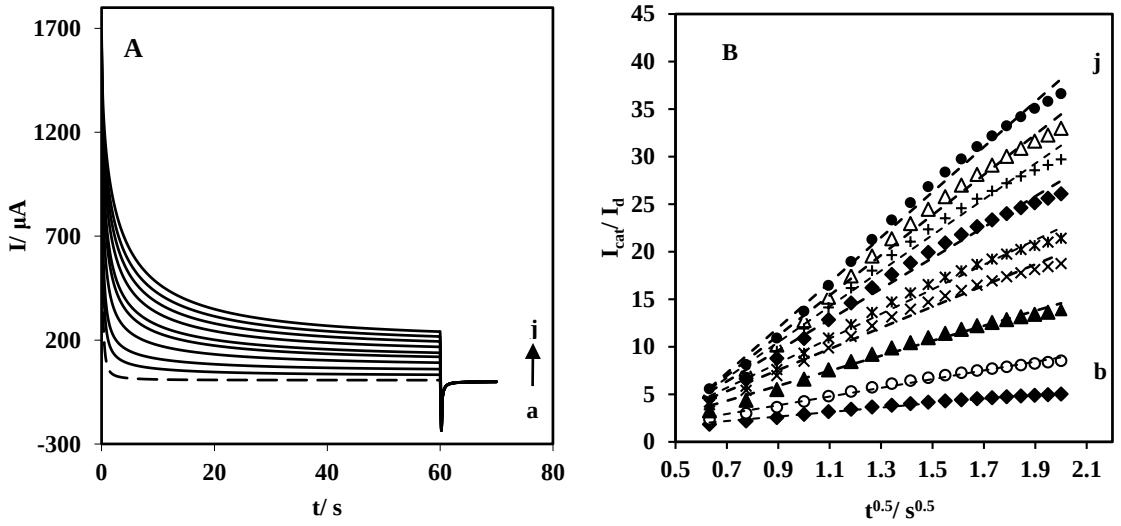

Fig. 7. (A) Chronoamperograms obtained at CSN- MCPE in the presence of different concentrations of cisapride; from bottom to top: 0.0, 1.0, 3.0, 5.0, 7.0, 9.0, 11.0, 13.0, 15.0, and 17.0 $\times10^{-6}$ mol L^{-1}; (B) Dependence of I_{cat}/I_d on $t^{1/2}$

3.7. Polarization Study

The pseudo-steady state polarization curves of the electrooxidation of cisapride on CSN-MCPE at a number of cisapride concentrations are presented in Fig. 8. The rotation rate of the electrode is maintained at 3000 rpm to avoid the interference of the mass transfer in the kinetics measurements. The oxidation process was found to begin at nearly 380 mV/Ag/AgCl and to reach a plateau at 583 mV/Ag/AgCl while the oxygen evolution starts at still higher potentials. In the course of reaction the coverage of Cu^{III} increases and reaches a saturation (steady state) level and the oxidation current follows accordingly. According to Eq. (3):

$$i = \left(\frac{2FAk_1\Gamma k_2 C_m}{k_1 + k_{-1} + 2k_2 C_m}\right) \quad (3)$$

Where A is the surface area of the electrode and the rate constants k_1 and k_{-1} of $Cu(II) \xleftrightarrow{k1,k-1} Cu(III) + e$ are obviously potential dependent and are of the forms:

$$k_1 = k^0{}_1 \exp\left[\frac{\alpha nFE}{RT}\right] \quad (4)$$

$$k_{-1} = k^0{}_{-1} \exp\left[\frac{(\alpha - 1)nFE}{RT}\right] \quad (5)$$

Where k^0's are the chemical rate constants measured at E/Ag, AgCl=0 with a being the anodic transfer coefficient and other parameters have their usual meanings.

The plots of the inverse current against the inverse cisapride concentration should be linear according to Eq. (6) [24]:

$$i^{-1} = (FAk_1\Gamma)^{-1} + \left[\frac{k_1 + k_{-1}}{2FAk_1k_2\Gamma}\right] C_m^{-1} \quad (6)$$

Fig. 9A presents i^{-1} versus C_m^{-1} dependencies where straight lines at various potentials have been obtained. Both the intercepts and slopes of the straight lines appearing in this figure were potential dependent. The slopes are plotted against exp(-nFE/RT) with n=1 and the graph is presented in Fig. 9B Using this graph along with Eq. (6) reveals that the rate constant of reaction, $k_2\Gamma(Cu^{III} + \text{analyte} \xrightarrow{k_2} \text{intermediate} + Cu^{II})$ and the ratio of $k^0{}_{-1}/k^0{}_1$ are 1.72×10^{-9} cm s^{-1} and 6.42×10^7 respectively. Where k^0's are the chemical rate constants measured at E/Ag, AgCl=0 with a being the anodic transfer coefficient and other parameters have their usual meanings. Fig. 9C presents the variation of the intercepts of the lines in Fig. 9A with the applied potential in a semi-log scale. Using this graph and Eq. (6) the magnitudes of $k_1^0\Gamma$ and the anodic transfer coefficient of 1.44×10^{-11} mol s^{-1} cm^{-2} and 0.4 have been obtained.

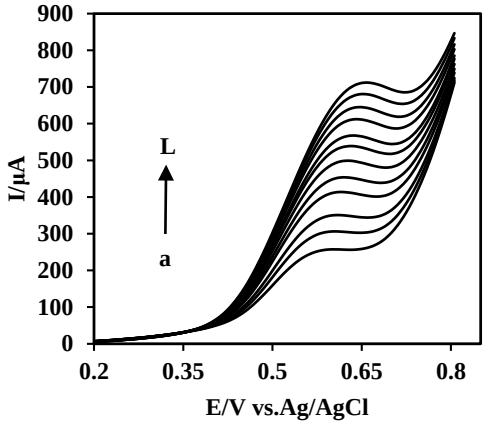

Fig. 8. Pseudo-steady state polarization curves of CSN- MCPE obtained in 7.0 (a), 9.0 (b), 11.0 (c), 13.0 (d), 15.0 (e), 17.0 (f), 19.0 (g), 21.0 (h), 23.0 (i), 25.0 (j), 27.0 (k) and 29.0 (l) $\times10^{-6}$ mol L^{-1} cisapride respectively. The potential sweep rate is 5 mVs^{-1}

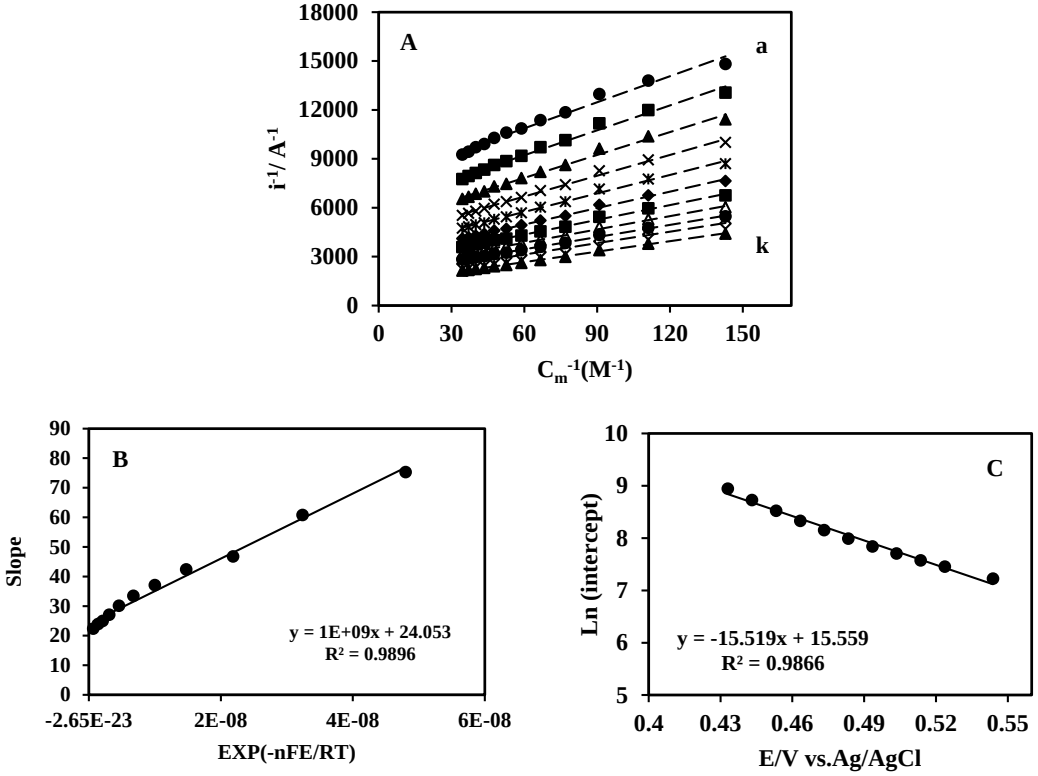

Fig. 9. (A) Plot of i^{-1} (from polarization curves in Fig. 8.) against C_m^{-1} at various potentials:(a) 433; (b) 443.1; (c) 453.2; (d) 463.3; (e) 473.3; (f) 483.4; (g) 493.5; (h) 503.5 ; (i) 513.6 (j) 523.7 and (k) 543.8 mV/Ag, AgCl as curves (a–k); (B) Plot of the slopes (of curves in 8A) *vs*. exp (-nFE/RT); (C) Plot of the Ln (intercepts) (of curves in 8A) *vs*. applied potential

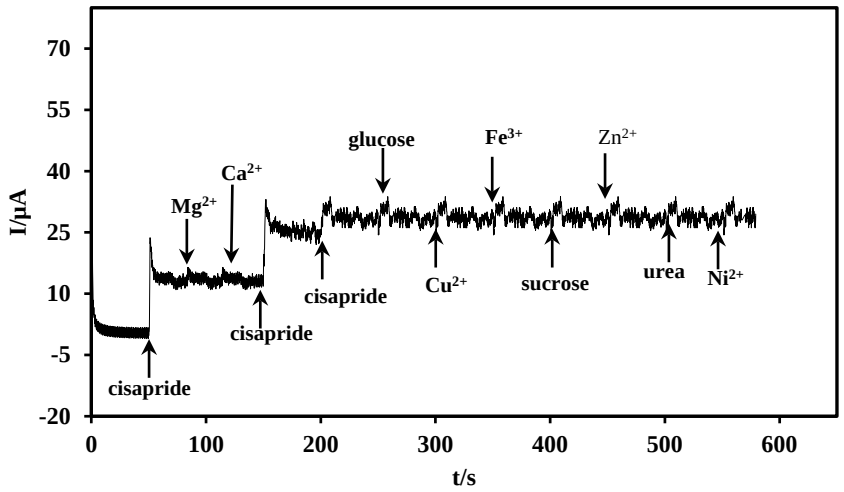

Fig. 10. Chronoamperometric responses for cisapride and interference of Mg^{2+}, Ca^{2+}, Ni^{2+}, Fe^{3+}, Cu^{2+}, Zn^{2+}, sucrose, glucose, and urea

3.8. Interference studies

The influence of various inorganic ions and organic compounds on the determination of cisapride (20×10^{-6} mol L^{-1}) was studied at optimum condition. The results showed that (Fig. 10)130-fold Mg^{2+}, Ca^{2+}, Ni^{2+}, Fe^{3+}; 80-fold Cu^{2+}, Zn^{2+}, sucrose, glucose, and urea did not interfere with the determination. The results proved that the proposed method had acceptable selectivity.

3.9. The repeatability and stability of the CSN-MCPE

The modified electrode exhibited a high stability. The relative standard deviation (R.S.D.) of five successive scans was 3.78% for 8×10^{-6} mol L^{-1} cisapride. Whenever it was placed in NaOH solution, only 3.48% loss of DPV current was found even after two month. The reproducibility of six independently fabricated electrodes showed a satisfactory value of 3.23% (R.S.D.).

3.10. Real sample analysis

Application of the proposed method was also tested by the analysis of cisapride tablets. Ten pieces of cisapride were powdered in a mortar, a portion of the resulting powder was accurately weighted and dissolved in methanol and diluted with water to appropriate concentration. The supernatant liquid was used for the determination of cisapride content by DPV method. Then, the standard addition method was used for determination of cisapride in the samples. The results show good quantitative recoveries (Table 2). This implied successful applicability of this method for real sample analysis

Table 2. Determination in cisapride tablets [a] by the proposed method

No.	Added (mg)	Expected (mg)	Found (mg)	Recovery (%)
1	0	5	4.89	97.80
2	5	10	9.93	99.30
3	10	15	14.80	98.67

[a] Each tablet contains 5 mg cisapride

4. CONCLUSION

In summary, in this paper, the kinetic of the electrocatalytic oxidation of cisapride at CSN-MCPE is demonstrated. The modified electrode has very good electrocatalytic activity. The electrochemical behavior of cisapride was greatly improved at the surface of CSN-MCP

electrode. High stability, good reproducibility, easy surface regeneration and fabrication are the important characteristics of the proposed electrode. The kinetics of the reaction has been developed and the magnitudes of the rate constants, anodic transfer coefficient of the electro-oxidation reaction have been obtained. The electrode had a long life time. The peak current and cisapride concentration show a linear relationship in a wide range.

REFEENCES

[1] J. E. F. Reynold, K. Parfitt, A. V. Parsons, and S. C. Martindale, in The Extra Pharmacopoeia, 32st ed, Royal Pharmaceutical Society of Great Britain, London (2002), pp. 879-880.
[2] J. C. Reynolds, and P. E. Putnam, Gastroenterol. Clin. North Am. 21 (1992) 567.
[3] L. R. Wiseman, and D. Faulds, Drugs. 47 (1994) 116.
[4] J. E. Belgaied, and H. Trabelsi, J. Pharm. Biomed. Anal. 33 (2003) 991.
[5] H. D. Janish, W. Hautteman, and M. H. Bonzo, Hepato-gastroenterology 35 (1988) 125.
[6] H. Geldof, B. Hazelhoff, and M. H. Otten, Aliment Pharmacol. Ther. 7 (1993) 409.
[7] S. Cisternino, J. Schlatter, and J. L. Saulnier, J. Chromatogr. B 714 (1998) 395.
[8] B. Dalmadi Kiss, K. Balogh Nemes and I. Klebovich, Chromatographia 57 (2003) 47.
[9] Z. Desta , N. V. Soukhova, A. Morocho, J. Park, S. K. Mahal, and D. A. Flockhart, J. Chromatogr. B 744 (2000) 263.
[10] M. I. G. Martin, C. G. Perez, and M. A. B. Lopez, Anal. Letts. 27 (1994) 1713.
[11] European Pharmacopoeia, fourth ed., Council of Europe, Strasbourg (2002).
[12] Z. Li, and S. Jun-Feng, Chin J. Anal. Chem. 35 (2007) 1018.
[13] I. G. Martin, C. G. Perez, and M. A. B. Lopez, Anal. Chim. Acta 368 (1998) 175.
[14] S. A. Ozkan, B. Uslu, and H. Y. Aboul-Enein, Crit. Rev. Anal. Chem. 33 (2003) 155.
[15] B. Uslu, and S. A. Ozkan, Anal. Lett. 44 (2011) 2644.
[16] B. Uslu, and S. A. Ozkan, Anal. Lett. 40 (2007) 817.
[17] H. R. Zare, and N. Nasirizadeh, Int. J. Electrochem. Sci. 4 (2009) 1691.
[18] K. I. Ozoemena, R. S. Staden, and T. Nyokong, Electroanalysis 21 (2009) 1651.
[19] S. Shahrokhian, and M. Amiri, Solid State Electrochem. 11 (2007) 1133.
[20] E. V. Ivanova, V. S. Sergeeva, J. Oni, Ch. Kurzawa, A. D. Ryabov, and W. Schuhmann, Bioelectrochem. 60 (2003) 65.
[21] M. Amiri, Z. Pakdel, A. Bezaatpour, and S. Shahrokhian, Bioelectrochemistry 81 (2011) 81.
[22] H. Song, H. Yin, N. Zhang, S. Li, B. Zhao, and K. Yu, Mater. Lett. 137 (2014) 56.
[23] A. Salimi, M. Roushani, and R. Hallaj, Electrochim. Acta 51 (2006) 1952.
[24] A. J. Bard, and L. R. Faulkner, Electrochemical Methods: Fundamentals and Applications; John Wiley & Sons: New York (2001).
[25] E. Laviron, J. Electroanal. Chem. 101(1979) 19.

[26] D. A. Skoog, F.J. Holler, T.A. Nieman, Principles of Instrumental Analysis, 5th ed. Harcourt Brace, Philadelphia (1998).